Femtosecond Coherent Control of Spins in (Ga,Mn)As Ferromagnetic Semiconductors Using Light

M. D. Kapetanakis and I. E. Perakis
Department of Physics, University of Crete, Heraklion, Crete 71003, Greece
Institute of Electronic Structure & Laser, Foundation for Research and Technology-Hellas, Heraklion, Crete 71110, Greece

K. J. Wickey and C. Piermarocchi
Department of Physics & Astronomy, Michigan State University, East Lansing, Michigan, 48824, USA

J. Wang
Department of Physics & Astronomy and Ames Laboratory-U.S. DOE, Iowa State University, Ames, Iowa 50011, USA
(Received 5 May 2009; published 24 July 2009)

Using density matrix equations of motion, we predict a femtosecond collective spin tilt triggered by nonlinear, near-ultraviolet (~3 eV), coherent photoexcitation of (Ga,Mn)As ferromagnetic semiconductors with linearly polarized light. This dynamics results from carrier coherences and nonthermal populations excited in the {111} equivalent directions of the Brillouin zone and triggers a subsequent uniform precession. We predict nonthermal magnetization control by tuning the laser frequency and polarization direction. Our mechanism explains recent ultrafast pump-probe experiments.

DOI: 10.1103/PhysRevLett.103.047404 PACS numbers: 78.47.J−, 42.50.Md, 78.20.Ls, 78.47.Fg

Long range magnetic order arises from the interactions between itinerant and localized spins in a wide variety of systems, such as EuO, EuS, chrome spinels, pyrochlore, manganese oxides, or (III,Mn)V ferromagnetic semiconductors [1,2]. With ferromagnetic semiconductors one can envision multifunctional devices combining information processing and storage on a single chip with low power consumption. Fast spin manipulation is of great importance for such spin-electronic, spin-photonic, magnetic storage, and quantum computation applications.

One of the challenges facing magnetic devices concerns their speed. The magnetic properties of carrier-induced ferromagnets respond strongly to carrier density tuning via light, electrical gates, or current [3]. While magnetic field pulses and spin currents can be used to manipulate spin on the many-picosecond time scale, femtosecond spin manipulation requires the use of laser pulses [4,5]. In ultrafast pump-probe magneto-optical spectroscopy, the pump optical pulse excites *e-h* coherences and corresponding carrier populations, whose subsequent interactions trigger a magnetization dynamics monitored as function of time via the Faraday or Kerr rotation [6].

The physical processes leading to femtosecond magnetization dynamics (femtomagnetism) are under debate. Open questions include the possibility of direct photon-spin coupling, the distinction of coherent and incoherent effects, and the exact role of the spin-orbit interaction. Following the pioneering work of Ref. [7], many ultrafast spectroscopy experiments were interpreted in terms of a decrease in the magnetization *amplitude* due to transient *thermal* effects [7,8]. Observations of light-induced changes in the magnetization *orientation* were also mostly attributed to the temperature elevation, which leads to transient changes in the magnetic easy axes [9–11]. Most desirable is *nonthermal* magnetization control within the femtosecond coherent [12] temporal regime, which promises more flexibility limited only by the optical pulse duration. Experiments in ferrimagnetic garnets were interpreted in terms of an interplay between the inverse Faraday effect [13] and long-lived changes in the magnetocrystalline anisotropy [4]. In (Ga,Mn)As, Ref. [14] reported magnetization precession triggered by changes of magnetic anisotropy on a ~100 ps time scale due to carrier relaxation, while Ref. [15] demonstrated coherent control of the precession. Recently, Wang *et al.* [5] observed *two* distinct temporal regimes of magnetization reorientation when (Ga,Mn)As is excited by 3.1 eV photons. Prior to the ~100 ps precession, they observed a *quasi-instantaneous* magnetization tilt, which was absent for excitation near the GaAs fundamental gap (~1.55 eV).

In this Letter we calculate the Mn spin dynamics triggered by femtosecond photoexcitation of (Ga,Mn)As with linearly polarized light. The joint density of states for interband transitions has a strong peak in the neighborhood of 3 eV, due to $\Lambda_3 \rightarrow \Lambda_1$ excitations along the eight equivalent directions {111} of the Brillouin zone (BZ), the Λ-edge [16]. Using a full tight-binding calculation of the bands, we show that photoexcitation at the Λ-edge is advantageous for nonthermal spin manipulation, due to the interplay between BZ symmetry, spin-orbit and magnetic exchange interactions, and coherent nonlinear photoexcitation. We predict a femtosecond temporal regime dominated by coherent *e-h* pairs and nonthermal populations. This is followed by a second regime determined by the

magnetic anisotropy of the Γ-point hole Fermi sea. We demonstrate magnetization control via the photoexcitation frequency and polarization direction and by changing the initial easy axis.

We use the Hamiltonian $H(t) = H_b + H_{\rm exch}(t) + H_L(t)$, where $H_b = H_0 + H_{\rm SO} + H_{\rm pd}$ describes the bands in the absence of photoexcitation [17]. H_0 describes the states in the presence of the periodic lattice potential, $H_{\rm SO}$ is the spin-orbit interaction, represented by on-site spin-dependent terms, while $H_{\rm pd}$ is the mean field interaction of the hole spin with the *ground state* Mn spin $\mathbf{S}_0$ (parallel to the easy axis) [2,18]. Here we focus on the metallic regime (hole densities $\sim 10^{20}$ cm^{-3}), where the virtual crystal approximation applies [2]. To describe the high momentum photoexcited states, we diagonalized H_b using the Slater-Koster sp^3s^* tight-binding Hamiltonian [19]. We thus obtained conduction electron states created by $\hat{e}^\dagger_{\mathbf{k}n}$, with energy $\varepsilon^c_{\mathbf{k}n}$, and valence hole states created by $\hat{h}^\dagger_{\mathbf{k}n}$, with energy $\varepsilon^v_{\mathbf{k}n}$. $\mathbf{k}$ is the crystal momentum and n labels the different bands. The holes experience an effective magnetic field colinear to $\mathbf{S}_0$, acting only on p-orbitals, which lifts the degeneracy of the heavy (hh) and light (lh) hole GaAs bands by the magnetic exchange energy $\Delta_{\rm pd} = \beta c S$, where c is the Mn density and S the Mn spin amplitude [2]. The interaction β is assumed independent of $\mathbf{k}$. In II-VI semiconductors, a direct theory-experiment comparison [20] suggested that β decreases along the Λ direction, likely due to the $\mathbf{k}$ dependence of the hybridization with Mn ions [21]. $H_{\rm exch}$ is the Kondo-like interaction between the hole spin and the photoexcited deviation, $\Delta\mathbf{S}$, of the Mn spin $\mathbf{S}$ from $\mathbf{S}_0$ [18]. The carrier coupling to the optical pulse is characterized by the Rabi energies $d_{mn\mathbf{k}}(t) = d_{mn\mathbf{k}} \exp[-t^2/\tau_p^2]$, where $\tau_p = 100$ fs is the pulse duration: [12]

$$H_L(t) = -\sum_{nm\mathbf{k}} d_{mn\mathbf{k}}(t)\hat{e}^\dagger_{\mathbf{k}m}\hat{h}^\dagger_{-\mathbf{k}n} + \text{H.c.} \tag{1}$$

We consider a linearly polarized optical field $\mathbf{E}(t)$ propagating along the [001] crystallographic axis (z axis). $d_{mn\mathbf{k}} = \mu_{mn\mathbf{k}}\mathbf{E}(t)$, where the dipole matrix elements $\mu_{mn\mathbf{k}}$ were expressed in terms of the tight-binding parameters [19] by considering the matrix elements of $\nabla_{\mathbf{k}} H_b(\mathbf{k})$ [22].

In addition to the photoexcited states, we consider the effect of the thermal holes. Wang *et al.* [8] measured an upper bound of ~200 fs to the hole spin relaxation time in InMnAs. The Fermi sea spin relaxes on a time scale of 10s of fs due to the interplay between disorder and spin-orbit [23] and other [8] interactions. For such fast relaxation, we assume to first approximation that the thermal hole spin adjusts adiabatically to the instantaneous $\mathbf{S}(t)$ [18] and describe the effects of the Fermi sea bath via its total energy $E_h(\mathbf{S})$ [17]. This Fermi sea populates valence states close to the Γ point. In view of uncertainties such as the population of impurity bands and the origin of strain [2,24], we adopt the general form of E_h dictated by the symmetry [17] and extract the anisotropy parameters from the experimental measurements [11,24]:

$$E_h = K_c(\hat{S}_x^2\hat{S}_y^2 + \hat{S}_x^2\hat{S}_z^2 + \hat{S}_y^2\hat{S}_z^2) + K_{uz}\hat{S}_z^2 - K_u\hat{S}_x\hat{S}_y. \tag{2}$$

The total energy E_h depends on the direction of the magnetization unit vector $\hat{\mathbf{S}}$ [17]. In contrast to magnetic insulators [4], the local Mn moments in (Ga,Mn)As are pure $S = 5/2$ spins with angular momentum $L = 0$, so the localized electrons do not contribute to the magnetic anisotropy. K_c is the cubic anisotropy constant, K_{uz} is the uniaxial anisotropy constant, due to strain and shape anisotropy, and K_u describes an in-plane uniaxial anisotropy observed experimentally [2,24]. Here we neglect for simplicity the light-induced temperature elevation and assume the equilibrium values of the anisotropy parameters [11,24]. For sufficiently large $K_{uz} > 0$, $\mathbf{S}_0$ lies within the x-y plane. For $0 < K_u < K_c$, as is the case at low temperatures, there are two in-plane metastable easy axes, X^- and Y^+ as in Ref. [5], which point at an angle ϕ, $\sin 2\phi = K_u/K_c$, with respect to the x axis [100] [24].

With ~3 eV photons, we excite high momentum states along the {111} equivalent directions in the BZ, which are well separated in energy from the thermally populated states [16]. We can then distinguish between thermal [25] and photoexcited carrier contributions to the mean field equation of motion of $\mathbf{S}(t) = \mathbf{S}_0 + \Delta\mathbf{S}(t)$,

$$\partial_t\mathbf{S} = -\gamma\mathbf{S}\times\mathbf{H}^{\rm th} - \frac{\beta}{V}\sum_{\mathbf{k}}\mathbf{S}\times\Delta\mathbf{s}^h_{\mathbf{k}} + \frac{\alpha}{S}\mathbf{S}\times\partial_t\mathbf{S}, \tag{3}$$

where γ is the gyromagnetic ratio, $\Delta\mathbf{s}^h_{\mathbf{k}}$ is the deviation (from its thermal value) of the total hole spin

$$\mathbf{s}^h_{\mathbf{k}} = \sum_{nn'}\mathbf{s}^h_{\mathbf{k}nn'}\langle\hat{h}^\dagger_{-\mathbf{k}n}\hat{h}_{-\mathbf{k}n'}\rangle, \tag{4}$$

α is the Gilbert damping coefficient [26], and $\mathbf{H}^{\rm th} = -\frac{\partial E_h}{\partial\mathbf{S}}$ is the thermal hole anisotropy field [25].

We describe the itinerant spin and charge dynamics within the mean field approximation by deriving equations of motion for the carrier populations and coherences [12]. The nonlinear e-h coherences are given by

$$\begin{aligned} i\partial_t\langle\hat{h}_{-\mathbf{k}n}\hat{e}_{\mathbf{k}m}\rangle = {} & (\varepsilon^c_{\mathbf{k}m} + \varepsilon^v_{\mathbf{k}n} - i/T_2)\langle\hat{h}_{-\mathbf{k}n}\hat{e}_{\mathbf{k}m}\rangle \\ & - d_{mn\mathbf{k}}(t)[1 - \langle\hat{h}^\dagger_{-\mathbf{k}n}\hat{h}_{-\mathbf{k}n}\rangle - \langle\hat{e}^\dagger_{\mathbf{k}m}\hat{e}_{\mathbf{k}m}\rangle] \\ & + \sum_{n'\neq n} d_{mn'\mathbf{k}}(t)\langle\hat{h}^\dagger_{-\mathbf{k}n'}\hat{h}_{-\mathbf{k}n}\rangle \\ & + \sum_{m'\neq m} d_{m'n\mathbf{k}}(t)\langle\hat{e}^\dagger_{\mathbf{k}m'}\hat{e}_{\mathbf{k}m}\rangle \\ & + \beta c\sum_{n'}\Delta\mathbf{S}(t)\cdot\mathbf{s}^h_{\mathbf{k}nn'}\langle\hat{h}_{-\mathbf{k}n'}\hat{e}_{\mathbf{k}m}\rangle. \end{aligned} \tag{5}$$

The nonlinear contributions to the above equation include phase space filling [12] (second line), coupling to carrier coherences (third line), and transient changes in the hole

states due to interactions with the light-induced $\Delta\mathbf{S}(t)$ (fourth line). The hole populations and intervalence band coherences are determined by the equation

$$
\begin{aligned}
i\partial_t\langle\hat{h}^\dagger_{-\mathbf{k}n}\hat{h}_{-\mathbf{k}n'}\rangle = (\varepsilon^v_{\mathbf{k}n'} - \varepsilon^v_{\mathbf{k}n} - i\Gamma^h_{nn'})\langle\hat{h}^\dagger_{-\mathbf{k}n}\hat{h}_{-\mathbf{k}n'}\rangle \\
+ \sum_m d^*_{mn\mathbf{k}}(t)\langle\hat{h}_{-\mathbf{k}n'}\hat{e}_{\mathbf{k}m}\rangle \\
- \sum_m d_{mn'\mathbf{k}}(t)\langle\hat{h}_{-\mathbf{k}n}\hat{e}_{\mathbf{k}m}\rangle^* \\
+ \beta c\sum_l \Delta\mathbf{S}(t)\cdot\mathbf{s}^h_{\mathbf{k}n'l}\langle\hat{h}^\dagger_{-\mathbf{k}n}\hat{h}_{-\mathbf{k}l}\rangle \\
- \beta c\sum_l \Delta\mathbf{S}(t)\cdot\mathbf{s}^{h*}_{\mathbf{k}nl}\langle\hat{h}^\dagger_{-\mathbf{k}l}\hat{h}_{-\mathbf{k}n'}\rangle, \qquad (6)
\end{aligned}
$$

while similar equations are obtained for the electrons. We note that the hole populations are coupled to the intervalence band coherences due to interactions with $\Delta\mathbf{S}(t)$. $\Gamma^h_{nn'}$, $n \neq n'$, are the dephasing rates and $\Gamma^h_{nn} = 1/T_1$ the population relaxation rate, which describe the photoexcited hole scattering and disorder or defect trapping effects.

We consider $\mathbf{S}_0$ parallel to an in–plane easy axis, X^- or Y^+ [5] ($S_z = 0$ initially [24]). Figures 1(a) and 1(d) show the femtosecond stage of the Mn spin dynamics triggered by a linearly polarized pulse tuned close to the Λ-edge with a fluence $\sim 7\ \mu\mathrm{J/cm}^2$ as in Ref. [5]. An out-of-plane magnetization tilt develops on this time scale, consistent with the experimental results for $\Delta\theta_K/\theta_K \approx \Delta S_z/S$ (inset), where θ_K is the Kerr rotation angle. This tilt practically disappears for $\sim$1.6 eV photoexcitation of corresponding states close to the Fermi surface [dashed curve in Fig. 1(b)]. For the anisotropy parameters of (Ga,Mn)As [11,24], the thermal contribution to Eq. (3), $\mathbf{H}^{\mathrm{th}}$, plays a minor role on the subpicosecond time scale. When the photoexcited hole dephasing and relaxation occurs faster than the pulse duration [Fig. 1(d)], $\Delta\mathbf{S}$ develops *during the optical excitation*, due to interactions with the coherent *e-h* pair spin. This initial dynamics is followed by a second temporal regime, Fig. 1(c), dominated by $\mathbf{H}^{\mathrm{th}}$ and characterized by zero-momentum magnon oscillations with frequency

$$\omega^2 = \frac{4\gamma^2}{S^2}\frac{K_c + K_{uz}}{K_c}(K_c^2 - K_u^2). \qquad (7)$$

If the hole relaxation is slower than the pulse duration, $\Delta\mathbf{S}(t)$ develops on a time scale $\sim T_1$, the population relaxation time [Figs. 2(a) and 2(b)]. We conclude that the femtosecond magnetization reorientation is governed by the dynamics of both coherent and nonthermal holes.

Because of its nonthermal origin, the femtosecond magnetization tilt can be controlled via the coherent photoexcitation. First, it increases with intensity. The *sign* of ΔS_z can be controlled by tuning the photoexcitation frequency, which controls which bands are excited, and by changing the direction of $\mathbf{S}_0$ [compare Figs. 1(a) and 1(b)]. Figure 1 demonstrates femtosecond resolution of the easy axis direction. Another means of control is demonstrated by Fig. 2, which shows the dependence of the tilt [Fig. 2(c)] and oscillations [Fig. 2(d)] on the direction of the optical field polarization as the latter is rotated within the *x-y* plane. An analogous effect was observed in ferrimagnetic garnets [4].

Similar to Ref. [18], our results can be interpreted in terms of photoexcitation of a pulsed hole spin component $\Delta\mathbf{s}^{h\perp}$ perpendicular to $\mathbf{S}_0$. Our mechanism should be contrasted to the inverse Faraday effect, which predicts that

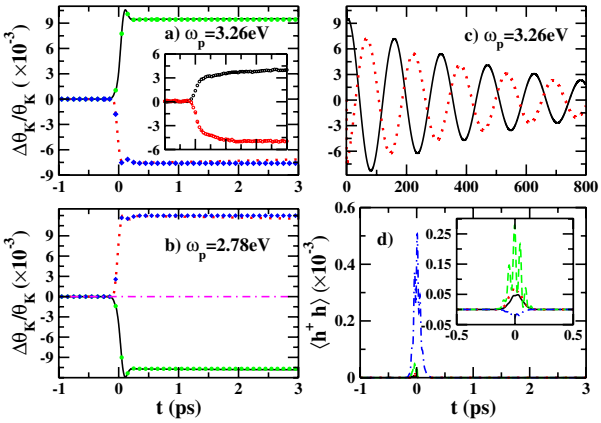

FIG. 1 (color online). Femtosecond Mn spin dynamics for hole relaxation faster than the optical pulse. (a) and (b): $\Delta S_z/S \approx \Delta\theta_K/\theta_K$ of the two in-plane magnetic memory states X^- (solid line) and Y^+ (dotted line) for two frequencies ω_p that excite different valence bands. Dashed-dotted curve in Fig. 1(b): $\omega_p = 1.6$ eV. Symbols: nonthermal dynamics ($\mathbf{H}^{\mathrm{th}} = 0$). Inset: Experiment [5] for X^- and Y^+, $\omega_p = 3.1$ eV. (c): Zero-$\mathbf{k}$ magnon oscillations following (a). (d): Populations and intervalence band coherences (inset) corresponding to (b). $\Delta_{\mathrm{pd}} = 130$ meV, $T_2 = 33$ fs, $K_c = 0.014$ meV, $K_u = K_c/3$, $K_{uz} = 5K_c$, $\alpha = 0.03$, $E = 2\times 10^5$ V/cm ($d \sim 0.6$–2 meV).

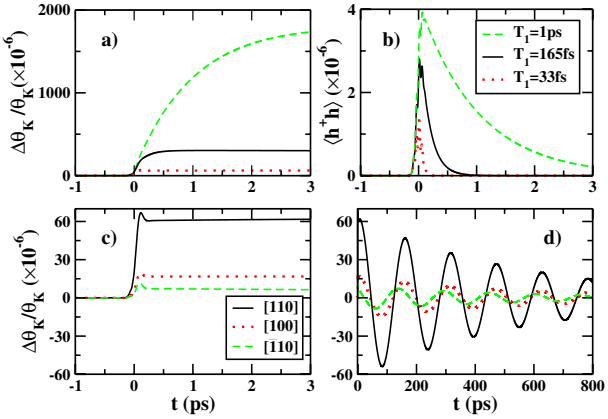

FIG. 2 (color online). (a): Femtosecond Mn spin dynamics for different T_1. (b) Hole population relaxation corresponding to (a). (c) and (d): Control, via the optical field polarization, of femtosecond dynamics (c) and zero-momentum magnon oscillations (d). $d \sim 0.1$ meV. Other parameters as in Fig. 1(a).

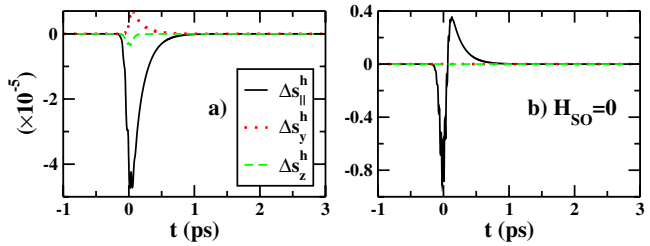

FIG. 3 (color online). Photoexcited total hole spin components parallel and perpendicular to $\mathbf{S}_0$: (a) Full calculation for the parameters of Fig. 2 (b) $H_{\mathrm{SO}} = 0$.

nonresonant excitation with circularly polarized light induces an effective magnetic field parallel to the direction of light propagation in a nonabsorbing material [13]. The interpetation of Ref. [13] relies on equilibrium concepts such as free energy. Here we develop a nonequilibrium theory that treats both interactions and coherent nonlinear optical effects similar to the Semiconductor Bloch equations [12]. Our theory describes the dynamics for both resonant and nonresonant photoexcitation and takes into account the quantum mechanical coherence between all bands. We may interpret $\Delta\mathbf{S}(t)$ as triggered by a *femtosecond* effective magnetic field pulse that does *not* point in the direction of light propagation.

We now turn to the role of the interactions H_{pd} and H_{SO} in photoexciting $\Delta\mathbf{s}^{h\perp}$. The hole spin, Eq. (4), is determined by the density matrices $\langle\hat{h}^{\dagger}_{-\mathbf{k}n}\hat{h}_{-\mathbf{k}n'}\rangle$, which can be simplified by expanding Eqs. (5) and (6) up to second order in the optical field, and by the spin matrix elements. H_{pd} and H_{SO} are characterized by the magnetic exchange, Δ_{pd}, and spin orbit, $\Delta_{SO} \sim 350$ meV, energies. In samples where $\Delta_{\mathrm{pd}} \gg \Delta_{\mathrm{SO}}$, the hole eigenstates are spin-polarized almost parallel to $\mathbf{S}_0$ for all $\mathbf{k}$, i.e., $\mathbf{s}^{h\perp}_{\mathbf{k}nn} \approx 0$. At the same time, the coherences $\langle\hat{h}^{\dagger}_{-\mathbf{k}n}\hat{h}_{-\mathbf{k}n'}\rangle$ are suppressed when $\varepsilon^{v}_{\mathbf{k}n'} - \varepsilon^{v}_{\mathbf{k}n}$ far exceeds the pulse frequency width, as for large Δ_{pd}. Figure 3 compares the calculated photoexcited spin components parallel ($\Delta\mathbf{s}^{h}_{\parallel}$) and perpendicular ($\Delta\mathbf{s}^{h}_{y}$ and $\Delta\mathbf{s}^{h}_{z}$) to $\mathbf{S}_0$ to the calculation with $H_{\mathrm{SO}} = 0$. $\Delta\mathbf{s}^{h\perp}$ is suppressed for $H_{\mathrm{SO}} = 0$ and therefore the light-induced femtosecond dynamics is heavily influenced by the (Ga,Mn)As valence band structure.

In the opposite limit $\Delta_{\mathrm{SO}} \gg \Delta_{\mathrm{pd}}$, the spin of the photoexcited hole states is almost parallel to $\mathbf{k}$, which points along the $\{111\}$ equivalent directions. The total $\Delta\mathbf{s}^{h}$ vanishes if all symmetric directions are excited equally. However, H_{pd} and the magnetic anisotropy break this symmetry and introduce a preferred direction along $\mathbf{S}_0$. The band energies now depend on the projection of $\mathbf{k}$ on $\mathbf{S}_0$. The linearly polarized optical field introduces another preferred direction that changes the Rabi energies $d_{mn\mathbf{k}}$. As a result, different $\mathbf{k}$ states are not photoexcited equally. Finally, for sufficiently small Δ_{pd}, the photoexcitation of intervalence band coherences becomes significant. Since in (Ga,Mn)As $\Delta_{\mathrm{pd}} \sim 150$ meV is comparable to Δ_{SO}, the spin dynamics results from a competition between H_{pd} and H_{SO} that must be treated numerically.

In summary, we developed a nonequilibrium theory of ultrafast magnetization reorientation in (Ga,Mn)As, triggered by the interactions of photoexcited coherences and nonthermal itinerant carriers with local Mn spins. We predict an initial femtosecond regime of spin dynamics and demonstrate non–thermalc magnetization control. Our calculations explain recent experiments [5].

This work was supported by the E.U. STREP program HYSWITCH, the U.S. National Science Foundation grant DMR0608501, and the U.S. Department of Energy-Basic Energy Sciences under contract DE-AC02-07CH11358.

[1] E. L. Nagaev, Phys. Rep. **346**, 387 (2001).
[2] T. Jungwirth *et al.*, Rev. Mod. Phys. **78**, 809 (2006).
[3] D. Chiba *et al.*, Nature (London) **455**, 515 (2008); J. Wang *et al.*, Phys. Rev. Lett. **98**, 217401 (2007).
[4] A. V. Kimel *et al.*, Nature (London) **435**, 655 (2005); F. Hansteen *et al.*, Phys. Rev. Lett. **95**, 047402 (2005).
[5] J. Wang *et al.*, Appl. Phys. Lett. **94**, 021101 (2009).
[6] J. Wang *et al.*, J. Phys. Condens. Matter **18**, R501 (2006); L. Cywiński and L. J. Sham, Phys. Rev. B **76**, 045205 (2007); E. Kojima *et al.*, Phys. Rev. B **68**, 193203 (2003).
[7] E. Beaurepaire *et al.*, Phys. Rev. Lett. **76**, 4250 (1996).
[8] J. Wang *et al.*, Phys. Rev. Lett. **95**, 167401 (2005).
[9] M. Vomir *et al.*, Phys. Rev. Lett. **94**, 237601 (2005).
[10] J. Qi *et al.*, Phys. Rev. B **79**, 085304 (2009); Appl. Phys. Lett. **91**, 112506 (2007).
[11] D. M. Wang *et al.*, Phys. Rev. B **75**, 233308 (2007).
[12] W. Schäfer and M. Wegener, *Semiconductor Optics and Transport Phenomena* (Springer-Verlag, Berlin, 2002).
[13] P. S. Pershan *et al.*, Phys. Rev. **143**, 574 (1966).
[14] Y. Hashimoto *et al.*, Phys. Rev. Lett. **100**, 067202 (2008).
[15] E. Rozkotová *et al.*, Appl. Phys. Lett. **93**, 232505 (2008).
[16] K. S. Burch *et al.*, Phys. Rev. B **70**, 205208 (2004).
[17] M. Abolfath *et al.*, Phys. Rev. B **63**, 054418 (2001); T. Dietl *et al.*, Phys. Rev. B **63**, 195205 (2001).
[18] J. Chovan, E. G. Kavousanaki, and I. E. Perakis, Phys. Rev. Lett. **96**, 057402 (2006); J. Chovan and I. E. Perakis, Phys. Rev. B **77**, 085321 (2008).
[19] P. Vogl *et al.*, J. Phys. Chem. Solids **44**, 365 (1983).
[20] D. Coquillat *et al.*, Phys. Rev. B **39**, 10 088 (1989).
[21] A. K. Bhattacharjee, Phys. Rev. B **41**, 5696 (1990).
[22] L. C. Lew Yan Voon and L. R. Ram-ohan, Phys. Rev. B **47**, 15 500 (1993).
[23] T. Jungwirth *et al.*, Appl. Phys. Lett. **81**, 4029 (2002).
[24] U. Welp *et al.*, Phys. Rev. Lett. **90**, 167206 (2003); X. Liu *et al.*, Phys. Rev. B **71**, 035307 (2005).
[25] J. R. MacDonald, Proc. Phys. Soc. London Sect. A **64**, 968 (1951).
[26] Y. Tserkovnyak, G. A. Fiete, and B. I. Halperin, Appl. Phys. Lett. **84**, 5234 (2004); M. D. Kapetanakis and I. E. Perakis, Phys. Rev. Lett. **101**, 097201 (2008).